Journal of Applied Polymer Science

Synthesis, characterization, thermal stability, and compatibility properties of poly(vinyl *p*-nitrobenzal acetal)-*g*-polyglycidylazides

Congdi Chen,[1] Bo Jin,[1] Rufang Peng,[1] Hengjian Huang,[2] Shijin Chu,[1] Haishan Dong[2]

[1]State Key Laboratory Cultivation Base for Nonmetal Composites and Functional Materials, Southwest University of Science and Technology, Mianyang 621010, China

[2]Institute of Chemical Materials, China Academy of Engineering Physics, Sichuan Mianyang 621900, China

Correspondence to: B. Jin (E-mail: jinbo0428@163.com) and R. Peng (E-mail: rfpeng2006@163.com)

ABSTRACT: A series of energetic polymers, poly(vinyl *p*-nitrobenzal acetal)-*g*-polyglycidylazides (PVPNB-*g*-GAPs), are obtained via cross-linking reactions of poly(vinyl *p*-nitrobenzal acetal) (PVPNB) with four different molecular weights polyglycidylazides (GAPs) using toluene diisocyanate as cross-linking agent. The structures of the energetic polymers are characterized by ultraviolet visible spectra (UV-Vis), attenuated total reflectance-Fourier transform-infrared spectroscopy (ATR-FT-IR), ^{1}H nuclear magnetic resonance spectrometry (^{1}H NMR), and ^{13}C nuclear magnetic resonance spectrometry (^{13}C NMR). Differential scanning calorimetry (DSC) is applied to evaluate the glass-transition temperature of the polymers. DSC traces illustrate that PVPNB-*g*−2$^{\#}$GAP, PVPNB-*g*−3$^{\#}$GAP, and PVPNB-*g*−4$^{\#}$GAP have two distinct glass-transition temperatures, whereas PVPNB-*g*−1$^{\#}$GAP has one. Thermogravimetric analysis (TGA) and differential thermal analysis (DTA) are used to evaluate the thermal decomposition behavior of the four polymers and their compatibility with the main energetic components of TNT-based melt-cast explosives, such as cyclotetramethylene tetranitramine (HMX), cyclotrimethylene-trinitramine (RDX), triaminotrinitrobenzene (TATB), and 2,4,6-trinitrotoluene (TNT). The DTA and TGA curves obtained indicate that the polymers have excellent resistance to thermal decomposition up to 200°C. PVPNB-*g*−4$^{\#}$GAP also exhibits good compatibility and could be safely used with TNT, HMX, and TATB but not with RDX. © 2015 Wiley Periodicals, Inc. J. Appl. Polym. Sci. **2015**, *132*, 42126.

KEYWORDS: copolymers; crosslinking; properties and characterization; thermal properties; thermogravimetric analysis (TGA)

Received 13 September 2014; accepted 16 February 2015

DOI: 10.1002/app.42126

INTRODUCTION

TNT-based melt-cast explosives, which are composed of TNT, RDX, or HMX explosives with aluminum metal, ammonium nitrate, and ammonium perchlorate oxidant, are obtained in molten state. These explosives are widely used in industrial and military applications because of their high detonation velocity, high power, thermal stability, adjustability to various shape chambers and so on.[1–3] However, melt-cast explosives exhibit poor mechanical properties and show undesirable defects, such as cracking, exudation, voiding, and brittleness, which can affect their ballistic performance and impact sensitivity.[4–6] These defects have motivated researchers to develop novel ways to obtain, use and store TNT-based melt-cast explosives without negative impacts to the explosives.[7–11] One useful method to improve the mechanical properties of TNT-based melt-cast explosives is addition of a proper amount of binders, such as polyvinyl formal, polyvinyl butyral, and polyvinyl acetate,[12–14] to the explosive mix. However, these are typically inert binders and their addition could reduce the energy of melt-cast explosives. Substitution of these inert binders with energetic binders may enhance the performance of such melt-cast explosives.

We recently reported an aromatic nitro polymer, poly(vinyl *p*-nitrobenzal acetal) (PVPNB), synthesized through the reaction of polyvinyl alcohol (PVA) with *p*-nitrobenzaldehyde.[15] PVPNB may present good compatibility with TNT and can be safely applied in TNT-based melt-cast explosives because both compounds share the same nitrophenyl group. We expect that PVPNB can enhance the mechanical properties of TNT-based melt-cast explosives. But the maximum condensation degree of PVPNB is 87% and its structure still has plenty of hydroxyl groups.[15] In order to boost energy level of PVPNB, more energetic groups should be grafted onto polymer molecule. The hydroxyl group can be easily modified through various reactions such as esterification, acetalization, etherification, and the like.[16–19] In the present study, PVPNB was further functionalized through cross-linking reactions with different molecular weight polyglycidylazides (GAPs) to obtain a series of energetic polymers called PVPNB-*g*-GAPs. These new energetic polymers

had feasible mechanical sensitivities, thermal stabilities and good compatibilities with the main energetic components of TNT-based melt-cast explosives, such as HMX, RDX, TNT and TATB.

EXPERIMENTAL

Materials

Dibutyltin dilaurate (DBTDL), toluene diisocyanate, *N*,*N*-dimethylacetamide (DMAC), dimethyl sulfoxide (DMSO), toluene, PVA (mean degree of polymerization 1700 ± 50, hydrolysis degree 99%), *p*-toluene sulfonic acid, and *p*-nitrobenzaldehyde were supplied by Chengdu Kelong Chemical Reagents Company. 1,2-dichloroethane was obtained from Chengdu Jinshan Chemical Reagent Company. All of the reagents and solvents were analytical grade and dried before use. Glycidyl azide polymers ($1^{\#}-4^{\#}$GAP) were provided by the Liming Chemical Engineering Research and Design Institute of Luoyang.

Synthesis

Synthesis of Poly(vinyl *p*-nitrobenzal acetal) (PVPNB). Up to 10.00 g of PVA (230.00 mmol —OH) was dissolved in 110 mL of dimethyl sulfoxide at 60°C under stirring. The reaction mixture was then heated to 90°C with stirring until the PVA was completely dissolved in the solvent. Subsequently, 0.90 g of *p*-toluene sulfonic acid and 17.20 g of *p*-nitrobenzaldehyde were added to the reaction mixture, which was stirred at 90°C for another 9 h. After completion of the reaction, the reaction mixture was poured into 500 mL of distilled water to precipitate the polymer. The polymer was washed several times with toluene and water and dried *in vacuo* at 50°C to obtain 23.20 g of the canary yellow solid PVPNB. The condensation degree of PVPNB was about 87%.[15]

Synthesis of Poly(vinyl *p*-nitrobenzal acetal)-*g*-polyglycidylazides (PVPNB-*g*-GAPs). PVPNB-*g*-GAPs were synthesized through cross-linking reactions of PVPNB with four different molecular weights GAPs using toluene diisocyanate as cross-linking agent. The general procedure is presented in Scheme 1.

Synthesis of Poly(vinyl *p*-nitrobenzal acetal)-*g*−1$^{\#}$polyglycidylazides (PVPNB-*g*−1$^{\#}$GAP). Exactly 4.41 g (25.00 mmol) of toluene diisocyanate, 0.30 g of DBTDL, and 20 mL of dried DMAC were placed in a 250 mL four-neck flask equipped with a condenser, mechanical stirrer and thermometer under high purity argon (99.99%) and then heated to 60°C. Up to 10.00 g of 1$^{\#}$GAP ($M_n = 623$, $M_w/M_n = 1.08$, hydroxyl value 142.2 mg/g, 25.00 mmol —OH) was then dissolved in 40 mL DMAC and added dropwise into the reaction solution. After stirring for 2 h, 10.00 g of PVPNB (dissolved in 40 mL of DMAC) was added to the reaction mixture, which was stirred at 60°C for another 24 h. Subsequently, the reaction mixture was poured into 1500 mL of distilled water.[20] The polymer was precipitated and separated out. The obtained polymer was washed with distilled water and then dried *in vacuo* at 50°C for 24 h to obtain 23.50 g of PVPNB-*g*−1$^{\#}$GAP, $M_n = 345400$, $M_w/M_n = 1.58$.

Synthesis of Poly(vinyl *p*-nitrobenzal acetal)-*g*−2$^{\#}$polyglycidylazides (PVPNB-*g*−2$^{\#}$GAP). Following the procedure for synthesizing PVPNB-*g*−1$^{\#}$GAP, 10.00 g of PVPNB was reacted with 1.20 g (6.90 mmol) of toluene diisocyanate and 10.00 g of 2$^{\#}$GAP ($M_n = 3068$, $M_w/M_n = 1.41$, hydroxyl value 38.7 mg/g, 6.90 mmol —OH) to obtain 20.02 g of PVPNB-*g*−2$^{\#}$GAP, $M_n = 348{,}220$, $M_w/M_n = 1.72$.

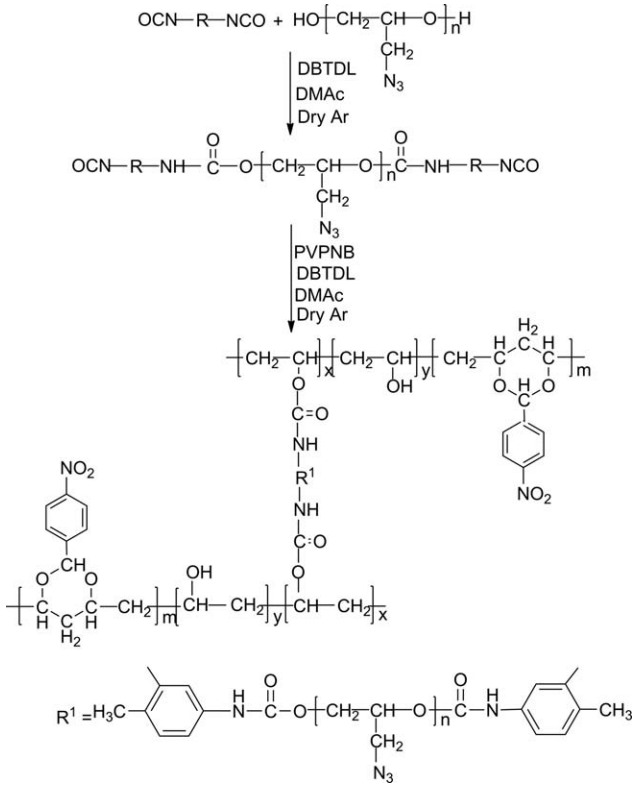

Scheme 1. Synthetic route of PVPNB-g-GAPs.

Synthesis of Poly(vinyl *p*-nitrobenzal acetal)-*g*−3$^{\#}$polyglycidylazides (PVPNB-*g*−3$^{\#}$GAP). Following the procedure for synthesizing PVPNB-*g*−1$^{\#}$GAP, 10.00 g of PVPNB was reacted with 0.55 g (3.14 mmol) of toluene diisocyanate and 10.00 g of 3$^{\#}$GAP ($M_n = 5031$, $M_w/M_n = 1.54$, hydroxyl value 17.6 mg/g, 3.14 mmol —OH) to obtain 19.60 g of PVPNB-*g*−3$^{\#}$GAP, $M_n = 350{,}430$, $M_w/M_n = 1.78$.

Synthesis of Poly(vinyl *p*-nitrobenzal acetal)-*g*−4$^{\#}$polyglycidylazides (PVPNB-*g*−4$^{\#}$GAP). Following the procedure for synthesizing PVPNB-*g*−1$^{\#}$GAP, 10.00 g of PVPNB was reacted with 0.70 g (4.05 mmol) of toluene diisocyanate and 10.00 g of 4$^{\#}$GAP ($M_n = 6990$, $M_w/M_n = 2.17$, hydroxyl value 22.7 mg/g, 4.05 mmol —OH) to obtain 19.80 g of PVPNB-*g*−3$^{\#}$GAP, $M_n = 353{,}410$, $M_w/M_n = 2.01$.

Characterization

ATR-FT-IR spectra were measured on Nicolet 6700 FT-IR spectrometer with a resolution of 4 cm^{-1} in the range of 4000-400 cm^{-1}.

UV-Vis spectra were recorded on UNICON UV-2102 PCS spectrometer using DMSO as solvent.

^{1}H NMR and ^{13}C NMR spectra were recorded on a Bruker Advance DRX 400 MHz instrument with hexadeuterated DMSO as solvent and tetramethylsilane as the internal reference.

DSC curves were characterized on a Q200 DSC instrument at a heating rate of 10°C/min in flowing high purity nitrogen

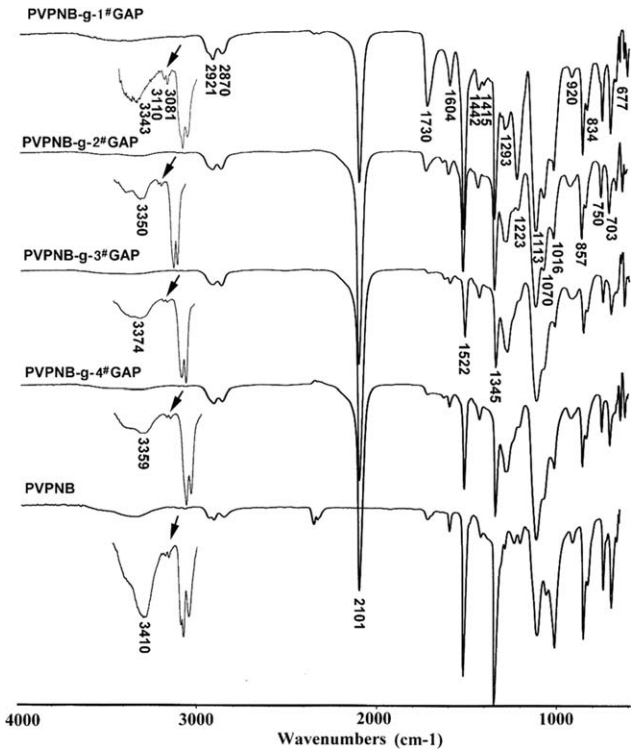

Figure 1. ATR-FT-IR spectra of PVPNB-*g*-GAPs and PVPNB.

(99.99%, flow rate 50 mL/min); T_g (glass-transition temperature) values were obtained from the DSC curves.

TGA was performed using an SDT Q600 TGA instrument with inflowing air (flow rate 50 mL/min) at a heating rate of 10°C/min.

DTA curves were recorded on a WCR-1B analyzer at a heating rate of 10°C/min, air atmosphere and Al_2O_3 as the reference.

The friction sensitivity was tested according to the national military standard GJB772A-97 602.1 method and the impact sensitivity was tested according to the national military standard method GJB772A-97 601.1 method.[21]

RESULTS AND DISCUSSION

Structural Analysis

The structures of PVPNB-*g*-GAPs were unambiguously assigned based on their ATR-FT-IR, UV-Vis, ^{1}H NMR, and ^{13}C NMR spectra.

The ATR-FT-IR spectra (Figure 1) showed changes in the chemical structures of original and modified PVPNBs. Characteristic adsorption peaks at 3110 and 3081 cm^{-1} in the IR spectra of PVPNB-*g*-GAPs were attributed to —CH stretching vibrations of the benzene rings (Figure 1). The band at 1730 cm^{-1} revealed the C═O group.[20] The strong and sharp absorption at 1522 cm^{-1} was attributed to the overlap of —NH flexural vibrations[22] and —NO_2 antisymmetric stretching vibrations. The peak at 1345 cm^{-1} was ascribed to —NO_2 symmetric stretching vibrations. Peaks at 1604 and 1442 cm^{-1} were attributed to aromatic ring skeleton stretching vibrations. The peak at 1223 cm^{-1} was assigned to the CO—O stretching vibration.[23] Bands at 1113 and 1016 cm^{-1} were related to acetal group C—O—C vibration coupling. The peak at 1070 cm^{-1} was identified as ester group C—O—C stretching vibrations. Bands at 857 and 750 cm^{-1} were also attributed to nitro group C—N stretching vibrations and C—N—O flexural vibrations. The peak at 834 cm^{-1} was ascribed to —CH out-of-plane flexural vibrations in the *p*-nitrobenzene ring. Compared with the IR spectrum of PVPNB, almost disappearance of the —OH stretching vibration peak was observed in the IR spectra of PVPNB-*g*-GAPs. A strong and sharp band observed at 2101 cm^{-1} was also attributed to —N_3 antisymmetric stretching vibrations and the peak at 1293 cm^{-1} was related to —N_3 symmetric stretching vibrations.[24] Analytical results of the ATR-FT-IR spectra indicated that PVPNB-*g*-GAPs were successfully synthesized from PVPNB and GAPs.

UV-Vis spectra of the PVPNB-*g*-GAPs were presented in Figure 2 (DMSO as solvent). The UV-Vis spectra showed a strong and broad absorption peak region at about 250 to 500 nm. PVPNB-*g*−1$^{\#}$GAP, PVPNB-*g*−2$^{\#}$GAP, PVPNB-*g*−3$^{\#}$GAP, and PVPNB-*g*−4$^{\#}$GAP showed maximum absorption peaks at 310, 306, 304, and 305 nm, respectively, owing to the nitrophenyl and azide groups of the copolymer side chain.[15,24] So the UV-Vis spectra analytical results strictly corroborated the ATR-FT-IR spectra analytical results that PVPNB-*g*-GAPs were successfully synthesized from PVPNB and GAPs.

The structure of PVPNB-*g*−1$^{\#}$GAP was also characterized by ^{1}H NMR and ^{13}C NMR spectra. Figure 3 showed the ^{1}H NMR spectrum of PVPNB-*g*−1$^{\#}$GAP. The signal at δ = 1.10–2.30 ppm was attributed to overlapping peaks of the methylene protons of the PVPNB main chain and the methyl protons of toluene diisocyanate (denoted a, d, f, and k). The signal at δ = 3.20–4.00 ppm was ascribed to overlapping peaks of the methine protons of the PVPNB main chain and the protons of GAP (—$OCH_2CH(CH_2N_3)O$—, denoted b, e, v, q and w). The signal at δ = 5.50–5.80 ppm indicated the proton of the PVPNB side chain (-OCHO-, denoted g). The signal at δ = 7.00–7.50 ppm corresponded to the benzene ring protons of toluene diisocyanate (denoted m, n, o).[25] Two broad signals at δ = 7.50–8.30 ppm were related the nitrophenyl ring protons of the side chain belonging to PVPNB (denoted i, h). The weak and broad signal at δ = 5.80–6.00 ppm was caused by hydroxyl groups in PVPNB (denoted c). The ^{13}C NMR spectrum of PVPNB-*g*−1$^{\#}$GAP was shown in Figure 4. The signal at about δ = 18.00 ppm was attributed to the methyl carbon of toluene diisocyanate (denoted k'). The signal at about δ = 44.64 ppm was ascribed to the methylene carbon of the PVPNB main chain (denoted a', d', f').[26] The signal at δ = 68.00–74.00 ppm was attributed to overlapping peaks of the methine carbon of the PVPNB main chain and the methine carbon of the GAP main chain (denoted b', e', w'). The signal at about 98.81 ppm was related to the carbon of the PVPNB side chain (—OCHO—, denoted g').[27] The signal at δ = 110.00–148.00 ppm was ascribed to the signal cross of nitrophenyl ring carbons of the PVPNB side chain and benzene ring carbons of toluene diisocyanate (denoted m', n', o', x', y', z', h', i', u', l'). Furthermore, the signal at δ = 153.00–155.00 ppm was related to the carbonyl carbon of PVPNB-*g*−1$^{\#}$GAP

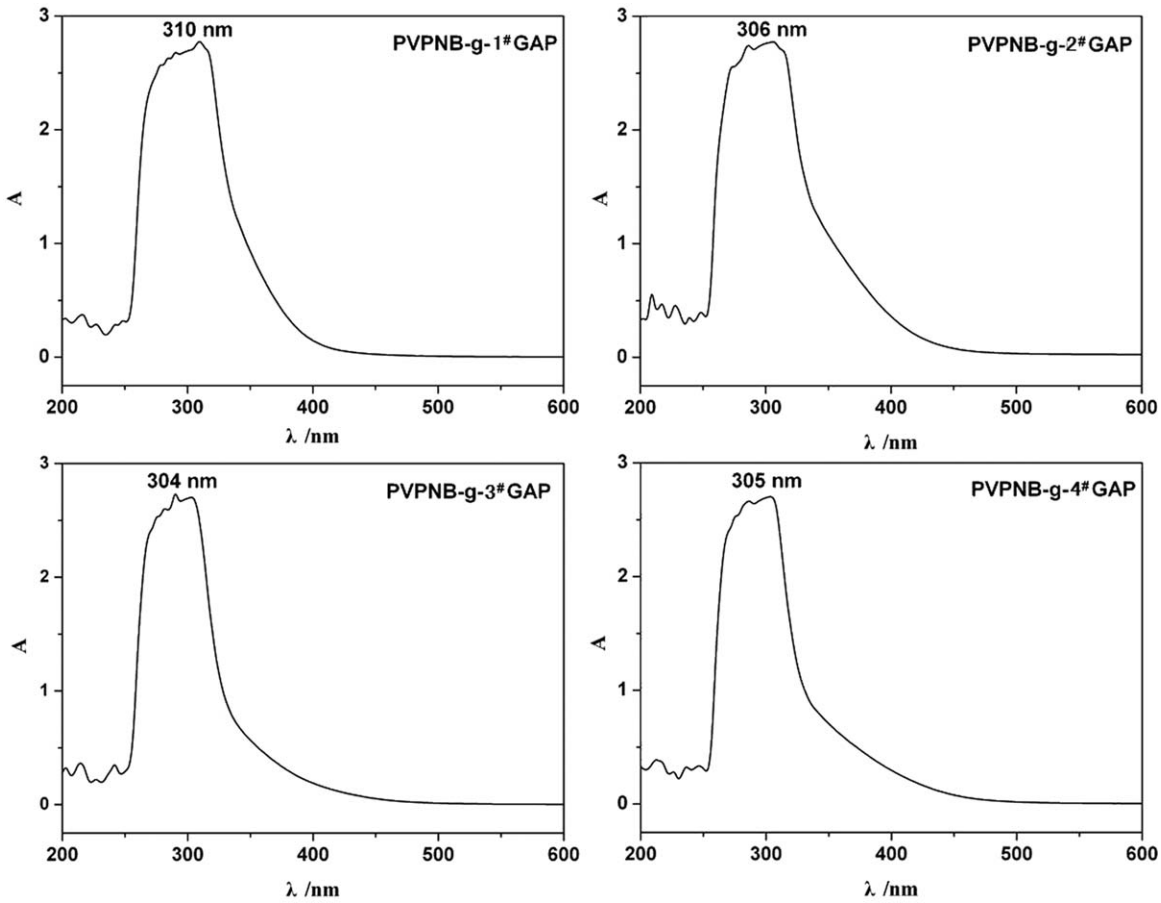

Figure 2. UV-Vis spectra of four PVPNB-*g*-GAPs.

(denoted p'). The signal at $\delta = 78.00–79.00$ ppm belonged to the ether bond carbon of the GAP main chain (—OCH_2—, denoted q').[28] The signal at $\delta = 51.00–52.00$ ppm was attributed to the azidomethyl carbon of the GAP side chain (—CH_2N_3, denoted v'). These signal positions observed in the ^{1}H NMR and ^{13}C NMR spectra of PVPNB-*g*−1$^{\#}$GAP strictly corroborated our ATR-FT-IR and UV-Vis analysis results.

Thermal Analysis

The thermal stability of energetic materials plays an important role in their preparation, processing, storage, and application. Thus, DTA was applied to study the thermal stability of the PVPNB-*g*-GAPs. The DTA curves (Figure 5) of the PVPNB-*g*-GAPs reflected excellent resistance to thermal decomposition up to 200°C. In addition, the compounds began to decompose gradually above the indicated temperature. All of the DTA curves exhibited three exothermic peaks. The first exothermic peak occurred at around 236°C, which was ascribed to decomposition of the azide group.[29] The second exothermic peak occurred at about 304°C, which was attributed to scission of side-chain nitrobenzene from PVPNB[30] and decomposition of the GAP main chain.[31] The third exothermic peak appeared at around 560°C and was attributed to decomposition of the PVPNB main chain.

Thermal characterization of the PVPNB-*g*-GAPs was further performed by recording their TGA and DTG curves. The TGA and DTG curves of the PVPNB-*g*-GAPs are presented in Figure 6; these curves all show three weight-loss temperatures under air atmosphere. Figure 6 (PVPNB-*g*−1$^{\#}$GAP) shows that the first weight-loss temperature began at 241°C, where about 22.27% of the polymer was lost. The second decomposition temperature began at 281°C with 28.06% weight loss. The final weight-loss peak occurred at 564°C with about 49.35% weight loss. The curves of PVPNB-*g*−2$^{\#}$GAP show decomposition

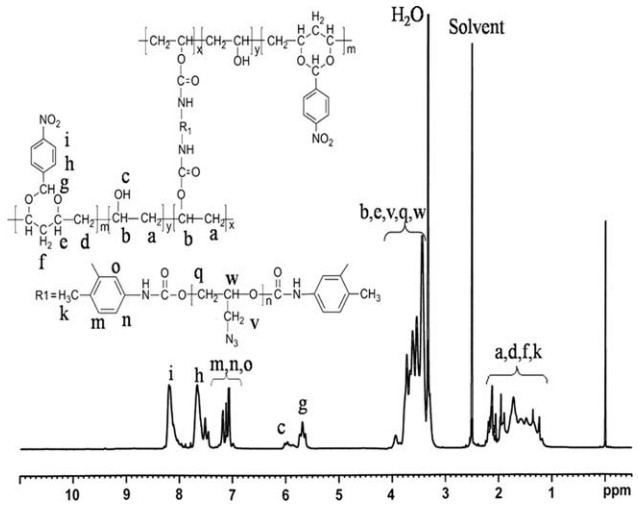

Figure 3. ^{1}H NMR spectrum of PVPNB-*g*−1$^{\#}$GAP.

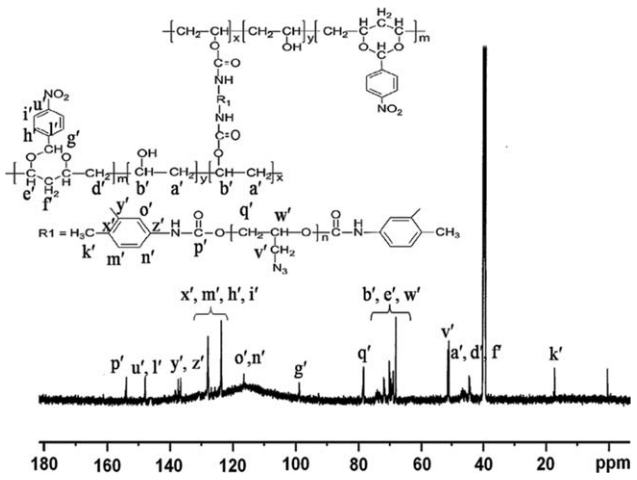

Figure 4. ^{13}C NMR spectrum of PVPNB-*g*−1$^{\#}$GAP.

temperatures: 247°C with 25.47% weight loss, 294°C with about 26.01% weight loss, and 577°C with 48.17% weight loss. Similarly, PVPNB-*g*−3$^{\#}$GAP, the first decomposition occurred at about 244°C, the second decomposition occurred at about at 294°C and the third decomposition occurred at about 566°C; weight losses at these temperatures were 23.70%, 28.02%, and 48.17%, respectively. Finally, in PVPNB-*g*−4$^{\#}$GAP, the first weight loss of 21.95% occurred at 240°C, the second weight loss of 28.29% occurred at 294°C, and the third weight loss of 49.90% occurred at 561°C. Comparing their first weight-loss temperatures, the stability of PVPNB-*g*−2$^{\#}$GAP is clearly superior to that of PVPNB-*g*−3$^{\#}$GAP, which, in turn, is more stable than PVPNB-*g*−1$^{\#}$GAP. PVPNB-*g*−4$^{\#}$GAP shows the most unstable features in all aspects.

To well understand the thermal decomposition mechanism of PVPNB-*g*-GAPs, thermogravimetric analysis tandem infrared spectrum (TGA-IR) was applied to rapidly identify the constituents of gaseous products during the decomposition of the most unstable copolymer PVPNB-*g*−4$^{\#}$GAP under nitrogen (Figure 7). As shown in Figure 7(a), TGA and DTG curves indicated the thermal degradation of PVPNB-*g*−4$^{\#}$GAP under nitrogen was a two-step reaction appeared at 248 and 305°C, respectively. Figure 7(b) depicted the FT-IR spectra of gaseous products during the decomposition of PVPNB-*g*−4$^{\#}$GAP at 248°C and 305°C. The results showed that the decomposed products of PVPNB-*g*−4$^{\#}$GAP at 248°C under nitrogen are mainly of N_2, CO_2 (2326 and 2300 cm^{-1}), CO (2155 and 2111 cm^{-1}), NH_3 (965 and 929 cm^{-1}), and NO_2 (1628 cm^{-1}). Therefore, the 22.97% mass loss observed in TGA curves of PVPNB-*g*−4$^{\#}$GAP at 248°C could be attributed to the breakdown of the azide group,[32] nitro group,[33] and urethane group.[34] The decomposed products of PVPNB-*g*−4$^{\#}$GAP at 305°C were mainly of CO_2 (2326 and 2286 cm^{-1}) and esters fragments (1791 and 1771 cm^{-1}).

To evaluate their thermal behavior further, glass-transition temperatures (T_g) were investigated by DSC (Figure 8). PVPNB-*g*−2$^{\#}$GAP, PVPNB-*g*−3$^{\#}$GAP, and PVPNB-*g*−4$^{\#}$GAP showed

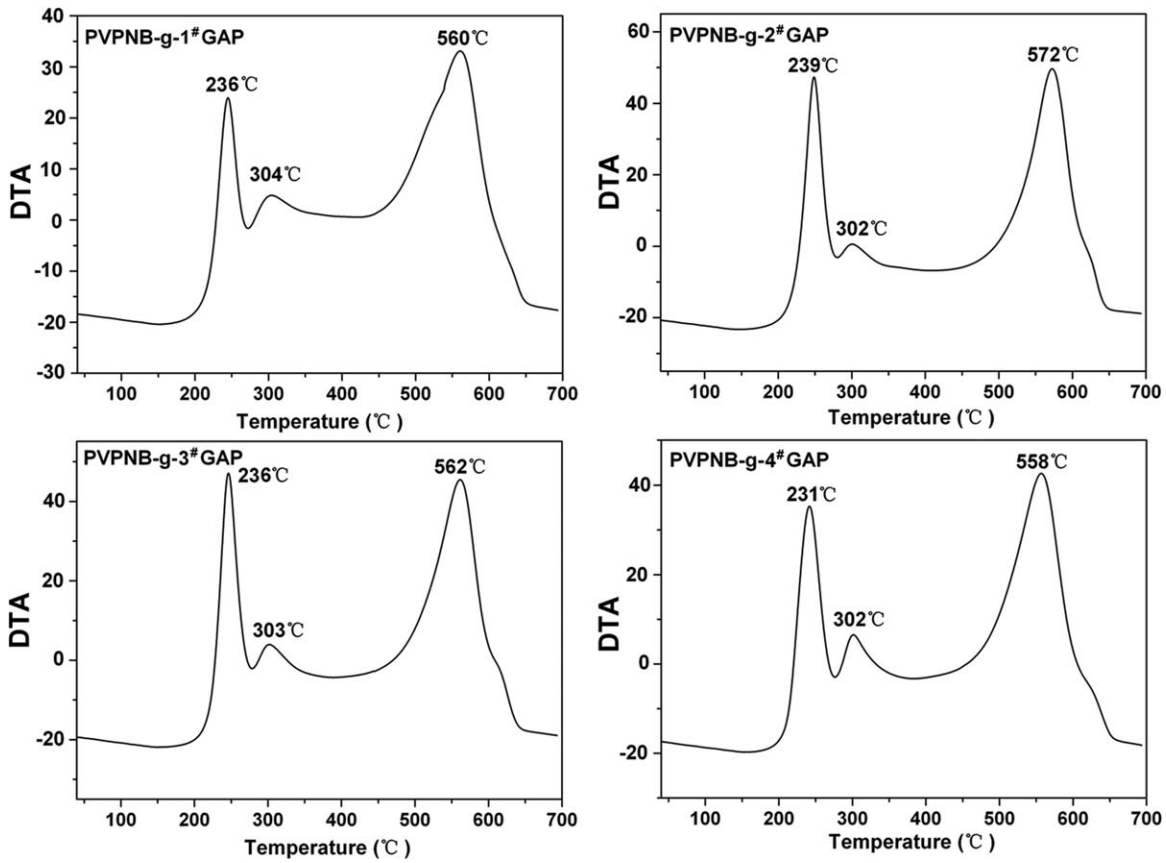

Figure 5. DTA curves of four PVPNB-*g*-GAPs.

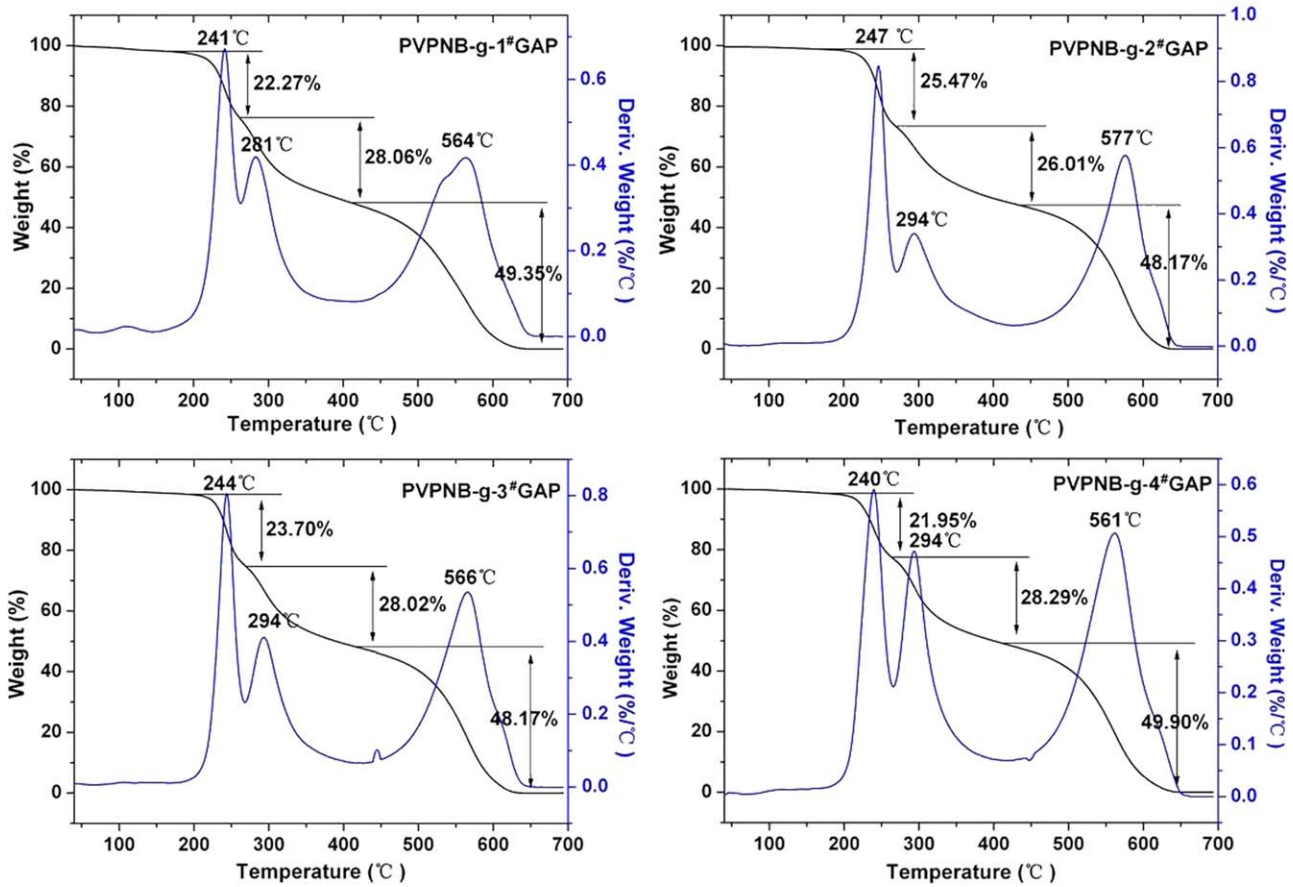

Figure 6. TGA and DTG curves of the four PVPNB-*g*-GAPs. [Color figure can be viewed in the online issue, which is available at wileyonlinelibrary.com.]

two distinct T_g at −38.96 and 10.85°C, −44.31 and 5.77°C, and −39.17 and 2.86°C, respectively. Whereas, PVPNB-g-1#GAP showed a single T_g at −3.91°C. The results indicated that PVPNB-*g*−2#GAP, PVPNB-*g*−3#GAP and PVPNB-*g*−4#GAP were biphasic system with the sub-microphase separation. The different T_g values were probably due to the interaction of incompatible segments of the blocks. Moreover, it revealed that PVPNB-*g*−1#GAP was a homogeneous phase system.[35–37]

Sensitivity Properties

The friction and impact sensitivities of PVPNB-*g*-GAPs were measured in accordance with national military standard method.[21] The testing conditions of friction sensitivity were

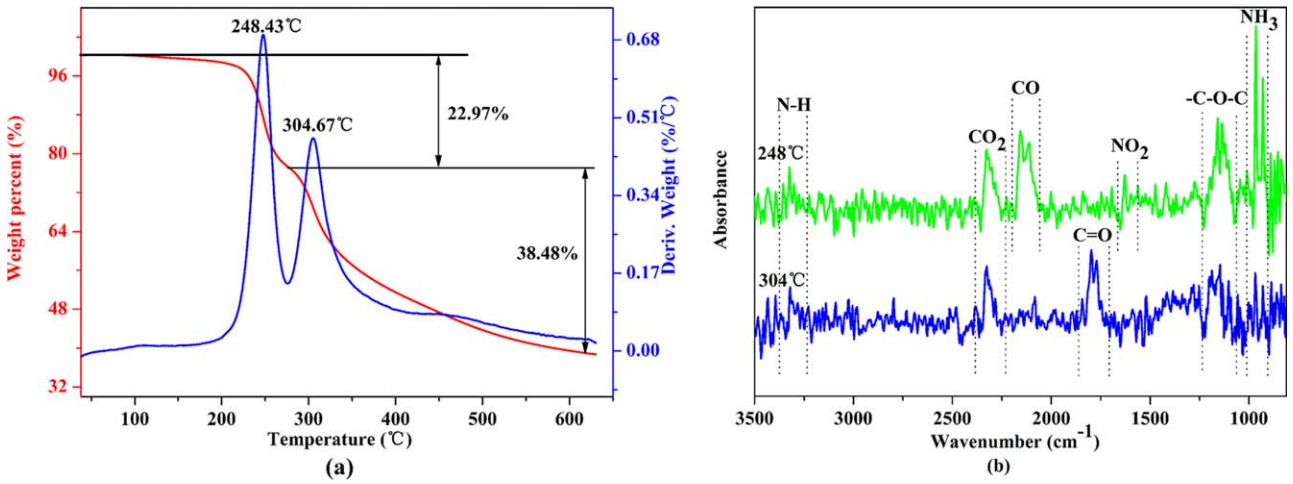

Figure 7. (a) TGA and DTG curves of PVPNB-*g*−4#GAP under nitrogen; (b) FT-IR spectra of gaseous products during the decomposition of PVPNB-*g*−4#GAP at 248°C and 305°C. [Color figure can be viewed in the online issue, which is available at wileyonlinelibrary.com.]

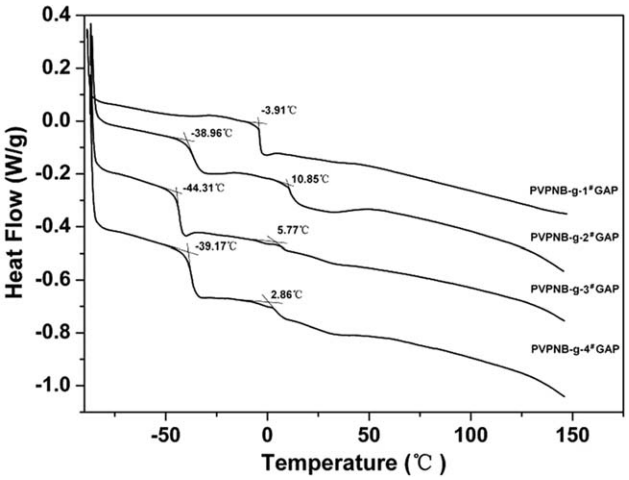

Figure 8. DSC curves of four PVPNB-*g*-GAPs.

that the weight of rocking hammer was 1.5 kg, the switch angle was 90°, the pressure was 3.92 MPa and the quantity of sample was 20 mg. Twenty-five samples were tested and the firing percent was calculated. The testing conditions of impact sensitivity were that the weight of dropping hammer was 10 kg, the height of dropping hammer was 25 cm and the quantity of sample was 50 mg. Twenty-five samples were tested and the firing percent was calculated. The results were shown in Table I. It showed that both the friction sensitivity and impact sensitivity of PVPNB-*g*-GAPs were lower than HMX and the order of friction sensitivity was HMX, PVPNB-*g*−2#GAP > PVPNB-*g*−1#GAP > PVPNB-*g*−3#GAP > PVPNB-*g*−4#GAP.

Table I. The Mechanical Sensitivities of PVPNB-*g*-GAPs

Sample	Friction sensitivity/%	Impact sensitivity/%
PVPNB-*g*−1#GAP	96	0
PVPNB-*g*−2#GAP	100	0
PVPNB-*g*−3#GAP	92	0
PVPNB-*g*−4#GAP	84	0
HMX[3]	100	100

Compatibility Testing

Compatibility is an important safety and reliability index used to evaluate the production, application and storage of energetic materials. DTA curves were used to determine the compatibility of PVPNB-*g*-GAPs with the main energetic components of TNT-based melt-cast explosives, such as HMX, RDX, TNT, and TATB, by investigating the effects of the contact materials on the exothermic decomposition temperature of the explosives.[38] Characteristic DTA curves of PVPNB-*g*−4#GAP and a mixture of PVPNB-*g*−4#GAP/TNT, PVPNB-*g*−4#GAP/HMX, PVPNB-

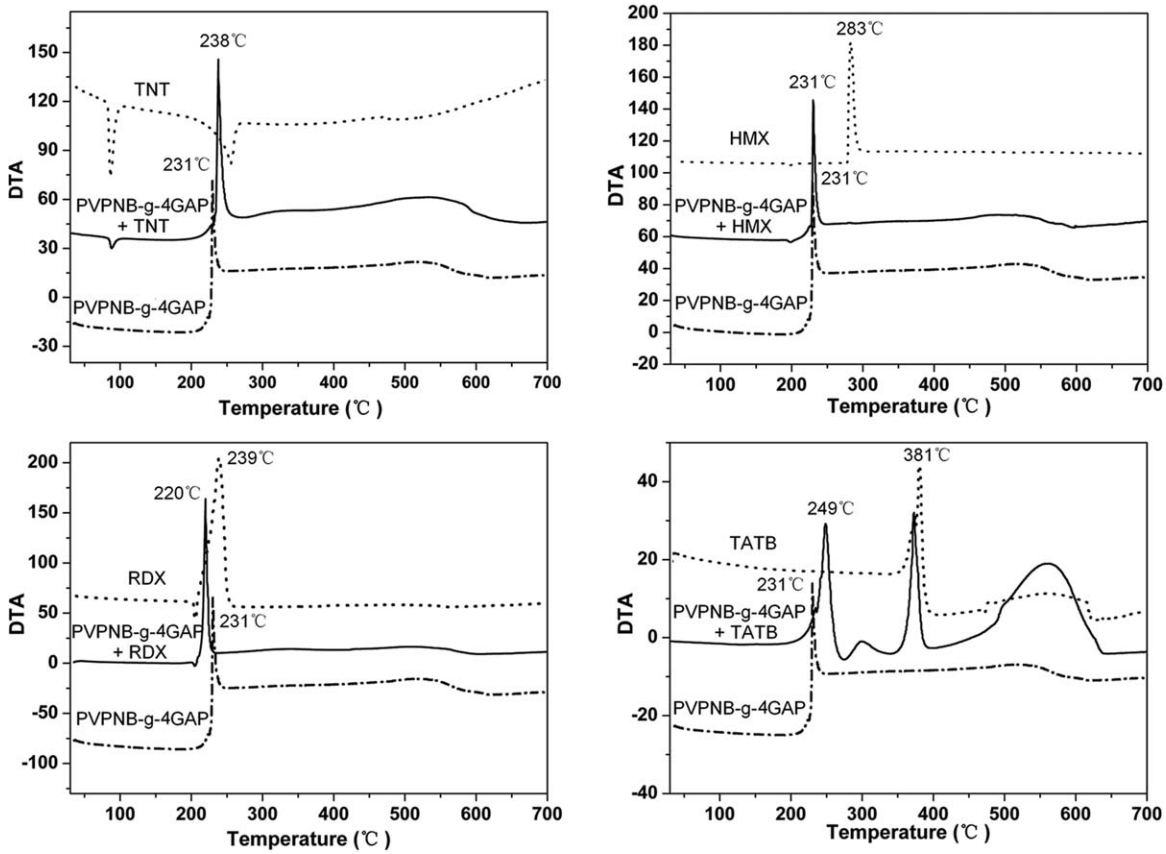

Figure 9. DTA curves of PVPNB-*g*−4#GAP and a mixture of PVPNB-*g*−4#GAP/TNT, PVPNB-*g*−4#GAP/HMX, PVPNB-*g*−4#GAP/RDX and PVPNB-*g*−4#GAP/TATB.

Table II. Maximum Exothermic Peak Temperatures and Maximum Exothermic Peak Temperature Differences ($\triangle T_p$) of PVPNB-*g*−4#GAP with TNT, HMX, RDX, and TATB

No.	Binary system	Single system	T_{p2} (°C)	T_{p1} (°C)	ΔT_p (°C)
1	PVPNB-*g*−4# GAP/TNT	PVPNB-*g*−4# GAP	238	231	−7
2	PVPNB-*g*−4# GAP/HMX	PVPNB-*g*−4# GAP	231	231	0
3	PVPNB-*g*−4# GAP/RDX	PVPNB-*g*−4# GAP	220	231	11
4	PVPNB-*g*−4# GAP/TATB	PVPNB-*g*−4# GAP	249	231	−18

g−4#GAP/RDX, and PVPNB-*g*−4#GAP/TATB were shown in Figure 9. The maximum exothermic peak temperatures and maximum exothermic peak temperature differences ($\triangle T_p$) (the maximum exothermic peak temperature of PVPNB-*g*−4#GAP single system subtracted the maximum exothermic peak temperature of binary system) of the compounds were also shown in Table II. Standards of compatibility for explosives and contacted materials[39] were listed in Table III. The $\triangle T_p$ between the PVPNB-*g*−4#GAP single system and PVPNB-*g*−4#GAP/TNT binary systems was −7°C (Figure 9 and Table II), while those between the PVPNB-*g*−4#GAP single system and the PVPNB-*g*−4#GAP/HMX, PVPNB-*g*−4#GAP/TATB, and PVPNB-*g*−4#GAP/RDX binary systems were 0, −18, and 11°C, respectively. According to standards of compatibility (Table III), the results in Table II indicated that the binary systems of PVPNB-*g*−4#GAP/TNT, PVPNB-*g*−4#GAP/HMX and PVPNB-*g*−4#GAP/TATB had good compatibility because their $\triangle T_p$ values were less than 2°C. Conversely, the $\triangle T_p$ of the binary system of PVPNB-*g*−4#GAP/RDX exceeded 2°C, which meant poor compatibility between PVPNB-*g*−4#GAP and RDX.

CONCLUSIONS

Four energetic polymers, PVPNB-*g*-GAPs, were synthesized by cross-linking four different molecular weights GAPs to PVPNB using toluene diisocyanate as the cross-linking agent. The structures of these compounds were confirmed by ATR-FT-IR, UV-Vis, ^{1}H NMR, and ^{13}C NMR and their thermal stability was estimated by DTA, TGA-DTG, and DSC. The DTA and TGA-DTG curves indicated that PVPNB-*g*-GAPs have excellent resistance to thermal decomposition up to 200°C and begin to decompose gradually at about 230°C. The DSC curves of PVPNB-g-2#GAP, PVPNB-g-3#GAP and PVPNB-g-4#GAP show two distinct T_g, whereas PVPNB-g-1#GAP shows only one. Moreover, sensitivity test and compatibility test results show that PVPNB-*g*−4#GAP is an insensitive material, which has good compatibility with TNT, HMX, and TATB. Further experiments will be carried out to demonstrate its capacity as a new energetic binder to improve the mechanical properties of TNT-based melt-cast explosives.

Table III. Standards of Compatibility for Explosives and Contact Materials

Criteria ($\triangle T_p$/°C)	Rating[a]	
Less than or equal to 2	A	Compatible or good compatibility
3 to 5	B	Slightly sensitized or moderate compatibility
6 to 15	C	Sensitized or poor compatibility
15 and above	D	Hazardous or bad compatibility

[a] A: safe for use in any explosive design; B: safe for use in testing, when the device will be used in a very short period of time, not to be used as a binder material, or when long-term storage is desired; C: not recommended for use with explosive items; D: hazardous, do not use under any conditions.

ACKNOWLEDGMENTS

The authors are grateful for financial support from the National Natural Science Foundation of China (Project No. 51372211), National Defense Fundamental Research Projects (Project No. A3120133002), Youth Innovation Research Team of Sichuan for Carbon Nanomaterials (2011JTD0017), Applied Basic Research Program of Sichuan Province (2014JY0170), and Southwest University of Science and Technology Researching Project (13zx9107).

REFERENCES

1. Sikder, A. K.; Sikder, N. *J. Hazard. Mater.* **2004**, *112*, 1.
2. Trzciński, W.; Cudziło, S.; Dyjak, S.; Nita, M. *Cent. Eur. J. Energy Mater.* **2014**, *11*, 443.
3. Dong, H. S.; Zhou, F. F. Performance of High Explosives and Correlates; Beijing: Science Press, **1989**.
4. Ravi, P.; Badgujar, D. M.; Gore, G. M.; Tewari, S. P.; Sikder, A. K. *Propell. Explos. Pyrot.* **2011**, *36*, 393.
5. Qian, W.; Shu, Y.; Li, H.; Ma, Q. *J. Mol. Model.* **2014**, *20*, 1.
6. Jadhav, P. M.; Sarangapani, R.; Ghule, V. D.; Prasanth, H.; Pandey, R. K. *J. Mol. Model.* **2013**, *19*, 3027.
7. Lin, M. J.; Ma, H. H.; Shen, Z. W.; Wan, X. Z. *Propell. Explos. Pyrot.* **2014**, *39*, 230.
8. Singh, A.; Kumar, M.; Soni, P.; Singh, M.; Srivastava, A. *Defence. Sci. J.* **2013**, *63*, 622.
9. Agrawal, J. P. *Prog. Energy Combust.* **1998**, *24*, 1.
10. Badgujar, D. M.; Talawar, M. B.; Asthana, S. N.; Mahulikar, P. P. *J. Hazard. Mater.* **2008**, *151*, 289.
11. Mohan, Y. M.; Raju, K. M. *Int. J. Polym. Anal. Chem.* **2004**, *9*, 289.
12. Eroğlu, M. S.; Hazer, B.; Güven, O.; Baysal, B. M. *J. Appl. Polym. Sci.* **1996**, *60*, 2141.
13. Pivovar, B. S.; Wang, Y.; Cussler, E. L. *J. Membr. Sci.* **1999**, *154*, 155.
14. Ulaganathan, M.; Pethaiah, S. S.; Rajendran, S. *Mater. Chem. Phys.* **2011**, *129*, 471.
15. Jin, B.; Peng, R. F.; Shen, J.; Tan, B. S.; Chu, S. J.; Dong, H. S. *Chem. Ind. Eng. Prog.* **2011**, *30*, 1285.

16. Gao, B. J.; Lu, J. H.; Zhuang, R. B.; Zhang, G. H. *J. Appl. Polym. Sci.* **2009**, *114*, 3487.
17. Mansur, H. S.; Sadahira, C. M.; Souza, A. N.; Mansur, A. A. *Mater. Sci. Eng. C* **2008**, *28*, 539.
18. Jin, B.; Dong, H. S.; Peng, R. F.; Shen, J.; Tan, B. S.; Chu, S. J. *J. Appl. Polym. Sci.* **2011**, *122*, 1643.
19. Jin, B.; Shen, J.; Peng, R. F.; Shu, Y. J.; Chu, S. J.; Dong, H. S. *Macromol. Res.* **2014**, *22*, 117.
20. Naghash, H. J.; Akhtarian, R.; Iravani, M. *Korean. J. Chem. Eng.* **2014**, *31*, 1281.
21. Jin, B.; Peng, R.; Chu, S.; Huang, Y.; Wang, R. *Propell. Explos. Pyrot.* **2008**, *33*, 454.
22. Tamami, B.; Yeganeh, H.; Koohmareh, G. A. *Iran. Polym. J.* **2005**, *14*, 785.
23. Prado, M. A.; Dias, G.; Carone, C.; Ligabue, R.; Dumas, A.; Roux, C. L.; Micoud, P.; Martin, F.; Einloft, S. *J. Appl. Polym. Sci.* **2015**, *132*, 41854.
24. Huang, T.; Jin, B.; Peng, R. F.; Chu, S. J. *Int. J. Polym. Anal. Chem.* **2014**, *19*, 522.
25. Paul, C. J.; Gopinathan Nair, M. R.; Neelakantan, N. R.; Koshy, P.; Idage, B. B.; Bhelhekar, A. A. *Polymer* **1998**, *39*, 6861.
26. Miyazaki, K.; Sato, H.; Kikuchi, S.; Nakatani, H. *J. Appl. Polym. Sci.* **2014**, *131*, 40760.
27. Migda, W.; Rys, B. *Magn. Reson. Chem.* **2004**, *42*, 459.
28. Kawamoto, A. M.; Diniz, M. F.; Lourenço, V. L.; Takahashi, M. F. K.; Keicher, T.; Krause, H.; Menke, K.; Kempa, P. B. *J. Aerosp. Technol. Manag.* **2011**, *2*, 307.
29. Pisharath, S.; Ang, H. G. *Polym. Degrad. Stab.* **2007**, *92*, 1365.
30. Yao, M.; Chen, L.; Peng, J. *Propell. Explos. Pyrot.* **2010**, *35*, 1.
31. Korobeinichev, O. P.; Kuibida, L. V.; Volkov, E. N.; Shmakov, A. G. *Combust. Flame* **2002**, *129*, 136.
32. Jin, B.; Shen, J.; Peng, R.; Shu, Y.; Tan, B.; Chu, S.; Dong, H. *Polym. Degrad. Stab.* **2012**, *97*, 473.
33. Cataldo, F.; Ursini, O.; Angelini, G. *Carbon* **2013**, *62*, 413.
34. Zhang, Z.; Wang, G.; Luo, N.; Huang, M.; Jin, M.; Luo, Y. *J. Appl. Polym. Sci.* **2014**, *131*, 40965.
35. Eroglu, M. S.; Hazer, B.; Güven, O. *Polym. Bull.* **1996**, *36*, 695.
36. Zhao, W. Z.; Cong, Y. H.; Zhang, B. Y.; Gu, W. M. *J. Appl. Polym. Sci.* **2014**, *131*, 40866.
37. He, M. J.; Zhang, H. D.; Chen, W. X.; Dong, X. X. Polymer Physics; Fudan University Press: Shanghai, **1983**.
38. Lee, J. S.; Jaw, K. S. *J. Therm. Anal. Calorimetry* **2006**, *85*, 463.
39. Yan, Q. L.; Li, X. J.; Zhang, L. Y.; Li, J. Z.; Li, H. L.; Liu, Z. R. *J. Hazard. Mater.* **2008**, *160*, 529.